

LII Zakopane School of Physics, International Symposium Breaking Frontiers, Zakopane, Poland, May 22–27, 2017

# Identification of Corrosion Products on Fe and Cu Metals using Spectroscopic Methods

D. ŚWIECH<sup>a,\*</sup>, C. PALUSZKIEWICZ<sup>b</sup>, N. PIERGIES<sup>b</sup>, E. PIĘTA<sup>b</sup>, U. LELEK-BORKOWSKA<sup>a</sup>  
AND W. KWIATEK<sup>b</sup>

<sup>a</sup>Faculty of Foundry Engineering, AGH University of Science and Technology,  
W.S. Reymonta 23, 30-059 Krakow, Poland

<sup>b</sup>Institute of Nuclear Physics, Polish Academy of Sciences, E. Radzikowskiego 152, 31-342 Krakow, Poland

In this study, the Fourier-transform infrared absorption and the Raman spectroscopies for analysis of corrosion products formed on the Fe and Cu metal surfaces after deposition in the chloride containing solution, were used. The obtained spectral patterns show that main constituent species of the corrosion products for Fe metal sample is lepidocrocite, while in the case of Cu surface there is formed mainly paratacamite. The obtained results confirm that application of vibrational spectroscopic methods is precise tool for identification and analysis of the corrosion products.

DOI: [10.12693/APhysPolA.133.286](https://doi.org/10.12693/APhysPolA.133.286)

PACS/topics: 33.20.Ea, 82.80.Gk, 42.55.Ye

## 1. Introduction

One of the most popular definition of corrosion is destroying a variety of materials (i.e. metals, alloys, concrete, glasses) that result from reaction with the corrosive environment [1]. The corrosion process depends on various factors, such as environment, pH, temperature, presence of the oxygen or aggressive ions in aqueous solution [1–3].

The very serious effects of the corrosion process generate problems of global significance. Many industries, such as energy, automotive, food, chemical, household appliances, brewery, suffer huge economic losses because of the corrosion damages [1, 4]. In order to prevent and control corrosion processes it is necessary to recognize and understand their mechanism. It can be achieved i.e. by detailed characterization of corrosion products.

Chloride ions present in many environments are very aggressive agent which can cause extensive corrosion of many materials [2, 5–7]. Chloride containing corrosion products are then very often detected on iron and copper objects [5–8].

Metals are constantly exposed to the natural environment and aggressive media (i.e. acids, bases and salts), thus many researchers have been involved in studies of the corrosion process in such media [5–8]. In the literature, the identification of the corrosion products is provided mainly by methods such as X-ray powder diffraction (XRD), X-ray photoelectron spectroscopy (XPS), scanning electron microscopy combined with an electron microprobe (SEM-EDS), less frequently infrared spectroscopy (IR) and the Raman spectroscopy (RS) [9–12].

The vibrational spectroscopic methods play an essential role in the examination of various structural constituents and can give complete, non-destructive identification of different compounds formed during corrosion processes [8, 12–14].

The present work focuses on the identification of the corrosion products formed on the Fe and Cu metals after exposition in the chloride containing solution by the Fourier transform infrared spectroscopy (FT-IR) and the Raman spectroscopy (RS).

## 2. Material and equipment

Metal samples such as Fe (purity 99.99%) and Cu (purity 99.99%) were investigated prior and after immersion in 1 M NaCl (Sigma Aldrich) solution prepared in deionized water (18 M $\Omega$ cm). The Fe and Cu samples were immersed simultaneously into the test solution and then measured after 0 h and 48 h of exposure. Before the measurements the metal samples (with size of 10 mm  $\times$  15 mm  $\times$  10 mm) were mechanically cleaned and rinsed in a ultrasonic bath with acetone and ethanol for 15 min each consequently. Then samples were washed with deionized water and dried.

FT-IR measurements were performed employing Vacuum FT-IR VERTEX 70V spectrometer with HYPERION 3000 IR microscope in combination with 15 magnification objective and MCT detector. In addition, Harrick Auto-Seagull accessory working with computer-controlled angle in the range of 45° and DTGS detector was used.

The Raman spectra were collected using the InVia Renishaw spectrometer equipped with: confocal Leica microscope and EMCCD detector (Back Illuminated, Deep Depletion CCD). The excitation wavelength was provided by a 632.8 nm laser with the power set at

\*corresponding author; e-mail: [dswiech@agh.edu.pl](mailto:dswiech@agh.edu.pl)

0.75 mW. All spectra were acquired with a spectral resolution of  $1\text{ cm}^{-1}$  in the spectral range of  $1700\text{--}100\text{ cm}^{-1}$ .

### 3. Results and discussion

The mapping area and FT-IR spectra collected for the Fe corroded sample after deposition in the NaCl solution are shown in Fig. 1. In Fig. 2A, the averaged FT-IR spectrum of the above mentioned corroded metal is presented. The most intense band at  $1021\text{ cm}^{-1}$  (in plane mode,  $\delta\text{-OH}$ ) in the FT-IR spectra of the corroded Fe sample (Figs. 1A and 2A) is due to the lepidocrocite ( $\gamma\text{-FeOOH}$ ) [8, 13]. The another bands at  $1153\text{ cm}^{-1}$  and  $740\text{ cm}^{-1}$  can be also attributed to OH deformations and bending in  $\gamma\text{-FeOOH}$  [8, 13]. The presence of the sharp bands around  $1021\text{ cm}^{-1}$  and  $740\text{ cm}^{-1}$  can suggest that the well crystallized phase of lepidocrocite is clearly present [14].

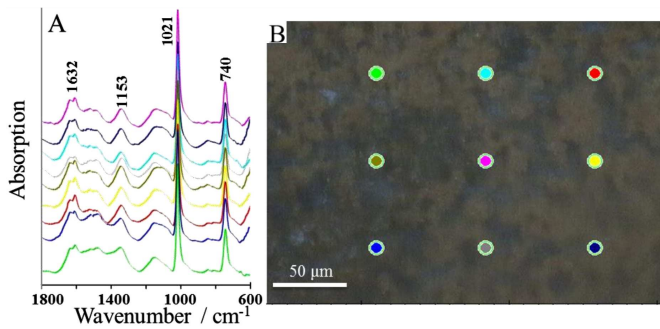


Fig. 1. The FT-IR spectra (A) and the mapping area (B) of Fe corroded sample at the selected points. Measurement conditions: spectral range  $1800\text{--}600\text{ cm}^{-1}$ , mapping area ( $195\text{ }\mu\text{m} \times 235\text{ }\mu\text{m}$ ), detector MCT.

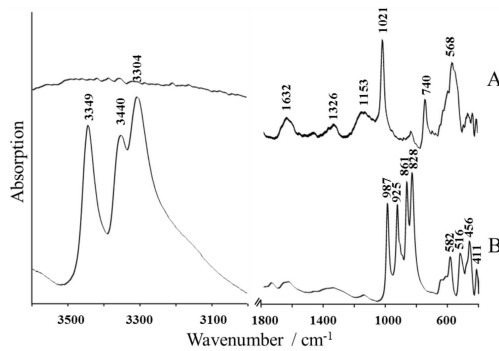


Fig. 2. The FT-IR spectra of Fe (A) and Cu (B) corroded samples. Measurement conditions: spectral ranges  $3600\text{--}3000$  and  $1800\text{--}400\text{ cm}^{-1}$ , reflection mode, the incident angle adjusted to  $45^\circ$ , detector DTGS.

The appearance of broad and strong intensity band at  $568\text{ cm}^{-1}$  with shoulder at  $665\text{ cm}^{-1}$  and  $445\text{ cm}^{-1}$  in the FT-IR spectrum of Fe sample (Fig. 2A) is resulted from the presence of magnetite ( $\text{Fe}_3\text{O}_4$ ) [15].

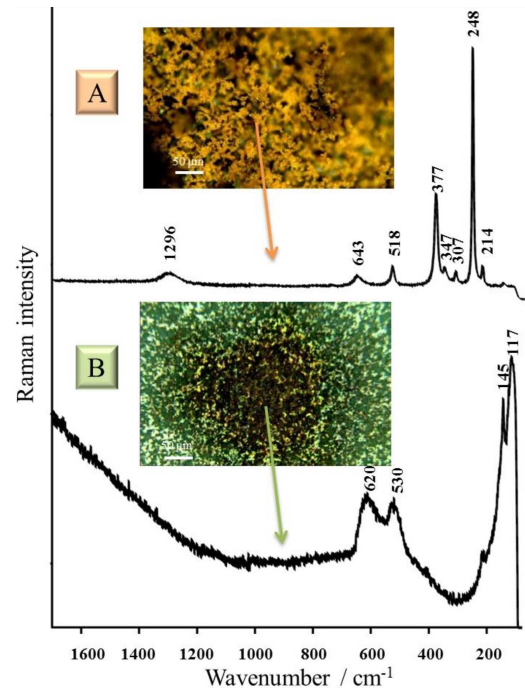


Fig. 3. The Raman spectra of Fe (A) and Cu (B) corroded samples at the marked point. Measurement conditions: spectral ranges  $1700\text{--}100\text{ cm}^{-1}$ , excitation wavelength  $632.5\text{ nm}$ .

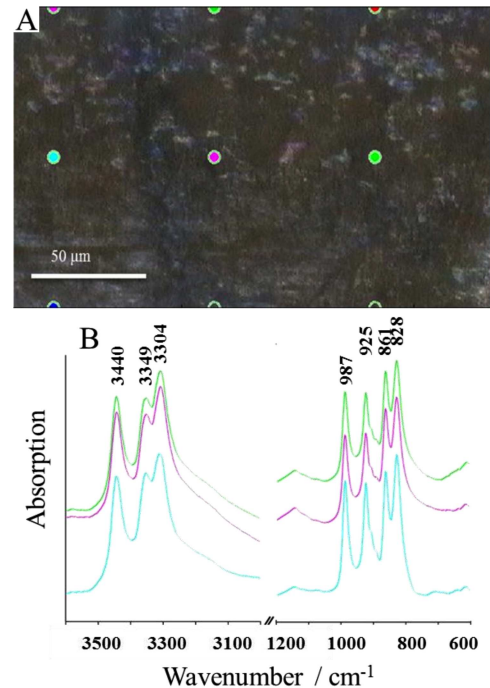


Fig. 4. The mapping area (A) and FT-IR spectra (B) of Cu corroded sample at the selected points. Measurement conditions: spectral ranges  $3600\text{--}3000$  and  $1200\text{--}600\text{ cm}^{-1}$ , mapping area ( $160\text{ }\mu\text{m} \times 195\text{ }\mu\text{m}$ ), detector MCT.

In addition, the broad absorption band at  $1632\text{ cm}^{-1}$  (Figs. 1A and 2A) can be assigned to OH bending vibrations in iron chloride containing compounds [12].

The Raman spectrum registered on the Fe corroded sample (Fig. 3A) is also dominated by the characteristic modes due to the lepidocrocite [16]. These modes appear at  $643, 518, 347, 248,$  and  $214\text{ cm}^{-1}$ , which indicates that the  $\gamma\text{-FeOOH}$  is predominant corrosion product. The appearance of the another band at  $307\text{ cm}^{-1}$  can be attributed to magnetite [17].

The formation of the above mentioned iron corrosion products facilitates appearance of cracks and loss of metal properties [13, 14].

The Cu exposed to humid air oxidises with formation of cuprite ( $\text{Cu}_2\text{O}$ ), which protects the surface against corrosion [6]. The fragment of layer corresponding to the  $\text{Cu}_2\text{O}$  (marked point — black area) is presented in Fig. 3B. In the Raman spectrum obtained on the Cu metal surface, the broad bands appearing at  $620\text{ cm}^{-1}$  and  $530\text{ cm}^{-1}$  are characteristic for  $\text{Cu}_2\text{O}$  (see Fig. 3B) [3].

Different phenomenon is observed for the FT-IR spectra of the Cu corroded sample. These spectra are dominated by modes of the paratacamite ( $\text{Cu}_2(\text{OH})_3\text{Cl}$ ) (Figs. 2B and 4B) [18, 19]. In the high wave number FT-IR spectral region ( $3440\text{--}3304\text{ cm}^{-1}$ ) of Cu surface the stretching vibrations of hydroxyl groups in paratacamite are strongly enhanced. In addition, in the lower wave number spectral range, bands occurring at  $987, 925, 861, 826\text{ cm}^{-1}$  are due to the Cu–O–H bending vibrations of  $\text{Cu}_2(\text{OH})_3\text{Cl}$  [18]. On the other hand, the absorbance bands at  $582, 516, 456,$  and  $411\text{ cm}^{-1}$  (see Fig. 2B) are characteristic for the Cu–O bending [20]. The presence of aggressive media such as chloride ions caused the breakdown of the passive  $\text{Cu}_2\text{O}$  film on the Cu metal surface due to the formation of species such as i.e.  $\text{CuCl}, \text{CuCl}_2^-$ . The  $\text{CuCl}_2^-$  ions can be oxidized to  $\text{Cu}_2(\text{OH})_3\text{Cl}$  [21, 22]. Paratacamite cannot provide good protection of the substrate due to its loose microstructure [6].

#### 4. Conclusions

In this work, analysis of the corrosion products formed on the Fe and Cu metal surfaces in the chloride containing solution was provided by means of the FT-IR and Raman spectroscopy techniques. The obtained results show that the dominant corrosion product for the Fe sample is lepidocrocite ( $\gamma\text{-FeOOH}$ ), while the Cu surface is covered mainly with paratacamite ( $\text{Cu}_2(\text{OH})_3\text{Cl}$ ). The results indicate that the vibrational spectroscopic methods are excellent tool for identification and analysis of the corrosion products at different positions on the metal surfaces.

#### Acknowledgments

The research was carried out using equipment purchased in the frame of the project co-funded by the

Małopolska Regional Operational Program Measure 5.1. Krakow Metropolitan Area as an important hub of the European Research Area for 2007–2013, project No. MRPO.05.01.00-12-013/15.

#### References

- [1] P.R. Roberge, *Handbook of Corrosion Engineering*, McGraw-Hill, New York 2000.
- [2] R.B. Comizzoli, R.P. Frankenthal, P.C. Milner, J.D. Sinclair, *Science* **234**, 340 (1986).
- [3] T. Kosec, Z. Qin, J. Chen, A. Legat, D.W. Shoesmith, *Corros. Sci.* **90**, 248 (2015).
- [4] R. Javaherdashti, *Anti-Corros. Method M.* **47**, 30 (2000).
- [5] G. Kear, B.D. Barker, F.C. Walsh, *Corros. Sci.* **46**, 109 (2004).
- [6] X. Liao, F. Cao, L. Zheng, W. Liu, A. Chen, J. Zhang, C. Cao, *Corros. Sci.* **53**, 3289 (2011).
- [7] Z.Y. Chen, D. Persson, A. Nazarov, S. Zakipour, D. Thierry, C. Leygraf, *J. Electrochem. Soc. B* **152**, 342 (2005).
- [8] Y. Takahashi, E. Matsubara, S. Suzuki, Y. Okamoto, T. Komatsu, H. Konishi, J. Mizuki, Y. Waseda, *Mater. Trans.* **46**, 637 (2005).
- [9] S.L. Wu, Z.D. Cui, F. He, Z.Q. Bai, S.L. Zhu, X.J. Yang, *Mater. Lett.* **58**, 1076 (2004).
- [10] J.J.S. Rodríguez, F.J.S. Hernández, J.E.G. González, *Corros. Sci.* **44**, 2425 (2002).
- [11] J. Duchoslav, R. Steinberger, M. Arndt, D. Stifter, *Corros. Sci.* **82**, 356 (2014).
- [12] B. Bozzini, G.P. De Gaudenzi, C. Mele, *Mater. Corros.* **54**, 694 (2003).
- [13] J. Weissenriederz, C. Leygraf, *J. Electrochem. Soc. B* **151**, 165 (2004).
- [14] D.C. Cook, A.C. Van Orden, J.J. Carpio, S.J. Oh, *Hyperfine Interact.* **113**, 319 (1998).
- [15] S. Musić, M. Gotić, S. Popović, *J. Mater. Sci.* **28**, 5744 (1993).
- [16] P. Colomban, in: *New Trends and Developments in Automotive System Engineering*, Ed. M. Chiaberge, InTech, Rijeka 2011.
- [17] A.M. Jubb, H. C. Allen, *ACS Appl. Mater. Inter.* **2**, 2804 (2010).
- [18] Z.Y. Chen, D. Persson, C. Leygraf, *J. Electrochem. Soc. B* **152**, 526 (2005).
- [19] R.L. Frost, *Spectrochim. Acta A* **59**, 1195 (2003).
- [20] A.R. Mendoza, F. Corvo, A. Gómez, J. Gómez, *Corros. Sci.* **46**, 1189 (2004).
- [21] H. Strandberg, L.G. Johansson, *J. Electrochem. Soc.* **145**, 1093 (1998).
- [22] M. Drogowska, L. Brossard, H. Menard, *J. Electrochem. Soc.* **139**, 39 (1992).